MODELLING VOLUMINOUS, RAPID LAVA FLOW EMPLACEMENT ON IO. A. G. Davies[1], L. Wilson[2], J. W. Head[3], K. de Kleer[4] and I. de Pater[5]. [1]Jet Propulsion Laboratory - California Institute of Technology, 4800 Oak Grove Drive, Pasadena, CA 91109, USA (Ashley.Davies@jpl.nasa.gov). [2]Lancaster University, Lancaster, Lancashire, UK. [3]Brown University, Providence, RI, USA. [4]California Institute of Technology, Pasadena, CA, USA. [5]University of California Berkeley, Berkeley, CA, USA.

Introduction: Io's voluminous and powerful "outburst" eruptions are characterised by lava fountains feeding extensive lava flows [1], an eruption style likely similar to that of ancient lunar eruptions [e.g., 2]. The processes that formed extensive, thick lava flows on the Moon and other bodies in their distant pasts are taking place now on Io. Io is the perfect place to understand how these eruptions behave.

Observations: Spacecraft observations, primarily from *Galileo*, have provided intermittent snapshots of this activity at moderate spatial resolution in the visible and infrared. Ground-based observations [3] (Figures 1 and 2) have provided more detailed temporal coverage, although at much lower spatial resolution. We are confident that these observations provide hard constraints on the emplacement mechanisms of lava flows, perhaps even to the extent of constraining the composition of the lava. Therefore, to maximize the extraction of information from these data we are developing physical models of eruptions in a vacuum to fit to the available data. The vast heat output from these most energetic eruptions is hard to understand unless high initial magma discharge rates generate fast-growing lava flows whose initial motion is fully turbulent.

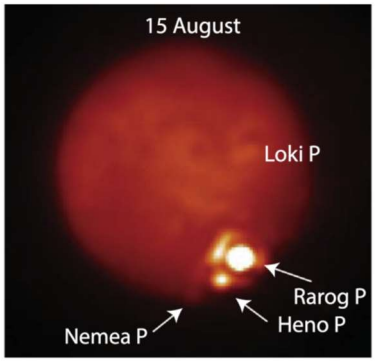

Figure 1. Two powerful (>10 TW) eruptions seen on Io on 2013 Aug 15 with the Keck telescope (shown at 2.2 μm) [3]. *These high-volume eruptions exhibited an exponential decay in thermal emission and emplaced lava over hundreds of km² in a few days.*

The Model: We have created and continue to refine a numerical model of flow emplacement (see flow chart, right). The model is currently in an Excel spreadsheet. We have run this model for initial end-member composition: a terrestrial tholeiitic basalt; and a 32% MgO komatiite. Our model (a) is designed for Io environment conditions; (b) tracks the growth of phenocrysts and the progressive onset of non-Newtonian rheology; (c) tracks the flow regime transition from turbulent to laminar using Reynolds (*Re*) and Hedstrom numbers; (d) is suitable for both basaltic and ultramafic compositions; (e) can be run for any fissure length; (f) fissure length can decrease as discharge decreases; (g) incorporates both steady and variable (Wadge-like) exponentially decreasing discharge rates (as end-members); and (h) incorporates variable initial peak discharge rate.

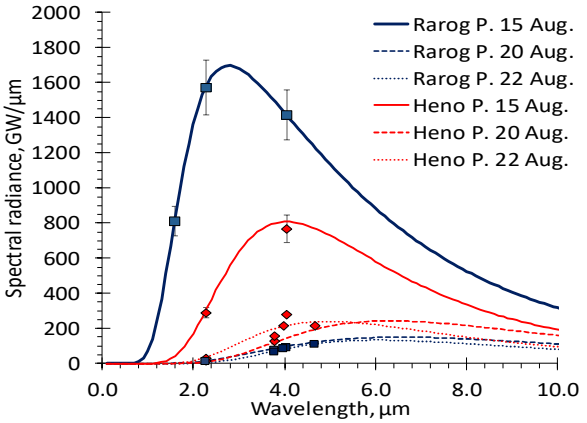

Figure 2. Evolution of the high-volume eruptions at Heno and Rarog Patera in August (after de Pater et al., 2014a). The temporal evolution of spectral radiance at different wavelengths is a strong constraint on the flow emplacement mechanism – and possibly lava composition.

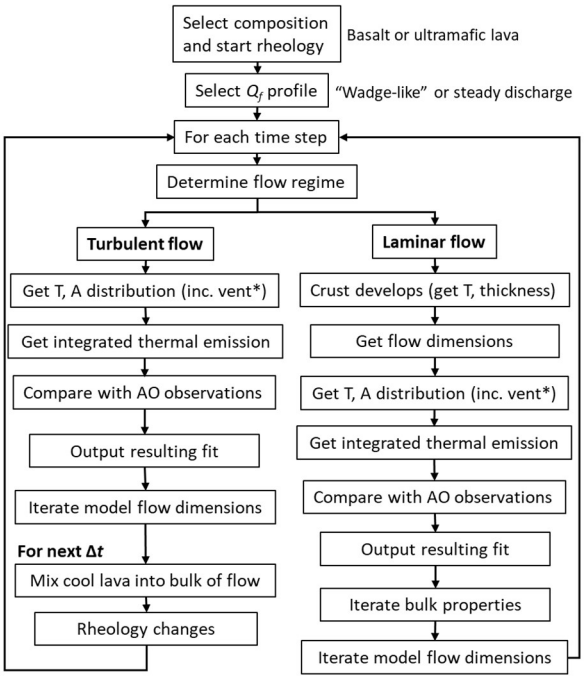

Figure 3. Model flow chart. (* = *optional*).

Model output: Figure 3 shows a comparison of the evolution of thermal emission with time for ultramafic and basalt flows for an initial lava discharge rate of 10^4 m^3/s and a decay constant of 1 day. The rapidly diverging trends suggest that compositional constraint is possible.

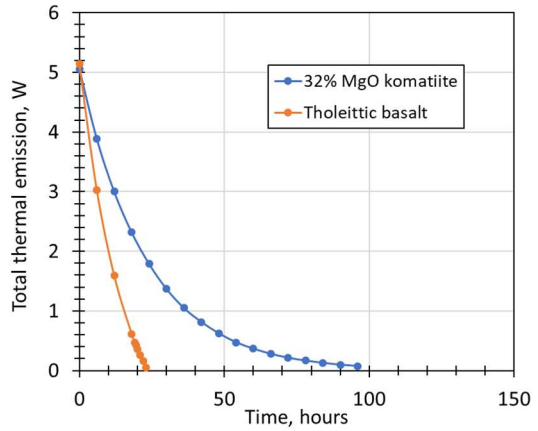

Figure 3. Comparison of total thermal emission from end-member composition cases for discharge rate of 10^4 m^3/s.

Tables 1 and 2 show the evolving flow parameters for end member compositions. In these examples, the fissure length, initially 1 km, is allowed to decrease at the same rate that the discharge rate decreases. This is analogous to actual fissure eruptions. The transition to laminar flow is faster for the basalt flow because of higher viscosity. Additionally, our initial calculations show that thermal emission from the levees that quickly form and rapidly cool is less than 1.5% of total thermal emission, even at its peak.

Table 1. Earth-like tholeiite

Time since start	Volume flux	Fissure length	Time to become laminar	Distance to laminar transition	Temp. of flow front lava at this time	Lava speed at laminar transition	Lava depth at laminar transition	Total radiant flux
/hours	/(m^3/s)	/km	/hours	/km	/K	/(m/s)	/m	/W
0	1.00E+04	1.000	0.840	8.88	1414	2.86	9.05	5.14E+12
6	7.79E+03	0.882	0.583	5.89	1418	2.75	8.35	3.03E+12
12	6.07E+03	0.779	0.361	3.48	1422	2.65	7.72	1.59E+12
18	4.72E+03	0.687	0.164	1.51	1426	2.54	7.13	6.14E+11
19	4.53E+03	0.673	0.130	1.18	1427	2.52	7.03	4.71E+11
19.5	4.44E+03	0.666	0.118	1.08	1427	2.52	6.99	4.24E+11
20	4.35E+03	0.659	0.100	0.91	1427	2.51	6.93	3.54E+11
21	4.17E+03	0.646	0.075	0.67	1428	2.49	6.85	2.59E+11
22	4.00E+03	0.632	0.047	0.42	1429	2.47	6.76	1.59E+11
23	3.84E+03	0.619	0.015	0.13	1430	2.46	6.65	4.90E+10
24	3.68E+03	0.607	not turbulent					

Discussions: (1) We find that to yield overall thermal emission of even a few TW from 1430 K tholeiitic basalt flows erupting from a long fissure (10 km) requires very high discharge rates exceeding 2 x 10^5 m^3/s, as lower discharge rates generate flows that are always laminar (see also [1] for a laminar flow example).

(2) With 1900 K 32% MgO ultramafic lavas, comparable high discharge rates yield considerably higher radiant fluxes as the flow remains turbulent for a longer period of time.

(3) When *Re* becomes less than Re_{crit} a rapid transition to laminar flow allows the growth of a cooling crust and cooling basal thermal boundary layer. For both initially low-viscosity and relatively high-temperature mafic and ultramafic lava compositions, the cool crust thickness is always less than the depth of the unsheared plug controlled by the yield strength. When the lower thermal boundary layer grows upward to meet the base of the plug, all motion ceases. *This is a very different basis for determining maximum flow length from the Gratz number criterion commonly used for flows that are laminar at all distances from the vent.*

Table 2. 32% MgO komatiite

Time since start	Volume flux	Fissure length	Time to become laminar	Distance to laminar transition	Temp. of flow front lava at this time	Lava speed at laminar transition	Lava depth at laminar transition	Total radiant flux
/hours	/(m^3/s)	/km	/hours	/km	/K	/(m/s)	/m	/W
0	1.00E+04	1.000	0.743	7.58	1789	2.79	3.51	5.06E+12
6	7.79E+03	0.882	0.678	6.59	1790	2.67	3.25	3.89E+12
12	6.07E+03	0.779	0.623	5.72	1792	2.55	3.01	3.00E+12
18	4.72E+03	0.687	0.569	4.99	1793	2.43	2.79	2.32E+12
24	3.68E+03	0.607	0.524	4.33	1794	2.32	2.58	1.79E+12
30	2.87E+03	0.535	0.472	3.76	1796	2.22	2.39	1.37E+12
36	2.23E+03	0.472	0.431	3.26	1798	2.11	2.21	1.05E+12
42	1.74E+03	0.417	0.396	2.84	1799	2.01	2.05	8.16E+11
48	1.35E+03	0.368	0.361	2.46	1801	1.92	1.89	6.26E+11
54	1.05E+03	0.325	0.325	2.10	1802	1.83	1.75	4.74E+11
60	8.21E+02	0.287	0.297	1.83	1804	1.75	1.62	3.66E+11
66	6.39E+02	0.253	0.270	1.58	1805	1.66	1.50	2.80E+11
72	4.98E+02	0.223	0.250	1.37	1806	1.59	1.39	2.14E+11
78	3.88E+02	0.197	0.223	1.18	1808	1.52	1.29	1.66E+11
84	3.02E+02	0.174	0.206	1.03	1809	1.45	1.20	1.27E+11
90	2.35E+02	0.153	0.188	0.89	1811	1.38	1.11	9.74E+10
96	1.83E+02	0.135	0.172	0.77	1812	1.31	1.03	7.50E+10

Next steps: This is a work in progress. The next steps are the generation of the evolving thermal emission spectra and comparison with the telescope observations to reduce parameter space. From our initial calculations, it appears that *composition and thermo-physical characteristics, combined with discharge rate, provide strong constraints on the resulting thermal emission peak and how thermal emission evolves with time*. This supports our approach. The ability to constrain lava composition from low spatial resolution multi-wavelength data would greatly advance our understanding of Io's magmatic processes, especially in light of new missions being planned to the Jovian system that would not necessarily pass close to Io, and with the continuing acquisition of data using ground-based telescopes.

Acknowledgements: This work was performed in part at the Jet Propulsion Laboratory-California Institute of Technology, under contract to NASA. © Caltech 2020. We thank the NASA Solar System Workings Program for support.

References: [1] Davies, A. G. (1994) *Icarus*, 124, 45-61. [2] Wilson, L. and Head, J. W. (2018) *GRL*, 45, 5852–5859. [3] de Pater, I. et al. (2014) *Icarus*, 242, 352-364.